



Minerva Access is the Institutional Repository of The University of Melbourne

Author/s:

Thomeer, LT;Guan, S;Gray, HA;Pandy, MG

Title:

Articular contact motion at the knee during daily activities

Date:

2022-08-01

Citation:

Thomeer, L. T., Guan, S., Gray, H. A. & Pandy, M. G. (2022). Articular contact motion at the knee during daily activities. *Journal of Orthopaedic Research*, 40 (8), pp.1756-1769. <https://doi.org/10.1002/jor.25222>.

Persistent Link:

<https://hdl.handle.net/11343/299275>

Shanyuanye Guan ORCID iD: 0000-0003-3717-4023

Hans Gray ORCID iD: 0000-0002-2587-8747

ARTICULAR CONTACT MOTION AT THE KNEE DURING DAILY ACTIVITIES

Lucas T. Thomeer, Shanyuanye Guan, Hans A. Gray, Marcus G. Pandy

Department of Mechanical Engineering, University of Melbourne, Parkville, Victoria
3010, Australia

REVISION 1

Submitted to Journal of Orthopaedic Research

31 August 2021

Author Contributions: LTT, HAG, SG, and MGP designed the study. MGP obtained funding for the research. LTT, SG, and HAG performed the data collection and analysis. LTT, SG, HAG and MGP interpreted the data and drafted the manuscript. All authors edited, revised, and approved the final version. MGP was the chief investigator for the study.

Corresponding author:

Marcus G. Pandy, Ph.D.

Department of Mechanical Engineering

The University of Melbourne

Parkville, Victoria 3010, Australia

email: pandym@unimelb.edu.au

This is the author manuscript accepted for publication and undergone full peer review but has not been through the copyediting, typesetting, pagination and proofreading process, which may lead to differences between this version and the [Version of Record](#). Please cite this article as [doi: 10.1002/jor.25222](https://doi.org/10.1002/jor.25222).

This article is protected by copyright. All rights reserved.

phone: +61 3 8344 4054; fax: +61 3 9347 8784

Running title: **Knee cartilage contact during activities**

ABSTRACT

We combined mobile biplane X-ray imaging and magnetic resonance imaging to measure the regions of articular cartilage contact and cartilage thickness at the tibiofemoral and patellofemoral joints during six functional activities: standing, level walking, downhill walking, stair ascent, stair descent, and open-chain (non-weight-bearing) knee flexion. The contact centers traced similar paths on the medial and lateral femoral condyles, femoral trochlea, and patellar facet in all activities while their locations on the tibial plateau were more varied. The translations of the contact centers on the femur and patella were tightly coupled to the tibiofemoral flexion angle in all activities ($r^2 > 0.95$) whereas those on the tibia were only moderately related to the flexion angle ($r^2 > 0.62$). The regions of contacting cartilage were significantly thicker than the regions of non-contacting cartilage on the patella, femoral trochlea, and the medial and lateral tibial plateaus in all activities ($p < 0.001$). There were no significant differences in thickness between contacting and non-contacting cartilage on the medial and lateral femoral condyles in all activities, except open-chain knee flexion. Our results provide partial support for the proposition that cartilage thickness is adapted to joint load and do not exclude the possibility that other factors, such as joint congruence, also play a role in regulating the structure and organization of healthy cartilage. The data obtained in this study may serve as a guide when evaluating articular contact motion in osteoarthritic and reconstructed knees.

Keywords: X-ray fluoroscopy, tibiofemoral, patellofemoral, cartilage thickness

INTRODUCTION

Cartilage plays a vital role in regulating joint health by reducing friction, increasing the articular contact area, and lowering joint stress. Altered bone motion can elevate joint stress and initiate cartilage degeneration^{1,2}. For instance, increased anterior tibial translation in the anterior-cruciate-ligament-deficient knee may shift load-bearing areas within the joint to regions of thinner cartilage where infrequent but excessive levels of stress occur³⁻⁵. Similarly, weakness of the quadriceps muscles can alter patellar tracking and overload cartilage in the patellofemoral compartment⁶. Accurate knowledge of cartilage contact locations across a range of daily activities would provide a better understanding of the effects of kinematic changes on cartilage health and inform current surgical and physiotherapy methods used to treat patients with joint instability and pain.

A number of studies have combined dynamic X-ray imaging with magnetic resonance imaging to determine the locations of articular contact at the knee⁷⁻¹³. Bingham et al.⁷ and Li et al.¹¹ measured the locations of contacting cartilage at the tibiofemoral (TF) joint as healthy individuals performed a forward lunge. Akpınar et al.¹² measured cartilage contact locations at the TF joint for the first 10% of the gait cycle in downhill walking and running, whereas Liu et al.⁸ measured TF cartilage contact locations for the entire stance phase of treadmill walking. Suzuki et al.¹³ measured cartilage contact locations at the patellofemoral (PF) joint during a step-up. No study thus far has measured cartilage contact at the TF or PF joint for complete cycles of daily activities, such as walking on level ground and walking up and down stairs and sloped surfaces.

Cartilage morphology is thought to be adapted to joint load^{1,2,4,14}. Findings that knee cartilage volume is positively correlated to physical activity during growth¹⁵, knee cartilage thickness increases after moderate running exercise¹⁶, and knee immobilization results in cartilage thinning¹⁷ support the view that the development and maintenance of cartilage are regulated by mechanical load. In contrast, Eckstein et al.¹⁸ examined the knees of well-trained triathletes and inactive controls and, finding no difference in cartilage thickness between the two groups, concluded that cartilage morphology may not be dependent on joint load. Differences in the results of these studies are difficult to reconcile because the locations of articular contact were not measured and only an average cartilage thickness was assessed.

A few studies have quantified cartilage thickness in the regions of articular contact at the knee. Li et al.¹¹ found that tibial and femoral cartilage thickness at the contact area in both the medial and lateral TF compartments during a forward lunge was 10 to 40% greater than the average cartilage thickness in healthy individuals. Liu et al.⁸ reported that the regions of TF contact during walking coincided with thicker cartilage covering the tibia but not the femur. Koo et al.¹⁹ and Scanlan et al.²⁰ found that the regions of TF contact at the beginning of the gait cycle (ipsilateral heel-strike) correlated with thicker cartilage on the medial femoral condyle but not the lateral femoral condyle or the tibial plateau. They measured cartilage thickness near ipsilateral heel-strike because this period of the gait cycle is associated with a high contact force acting at the knee. However, high contact forces are also transmitted by the TF joint near contralateral toe-off and contralateral heel-strike at ~10% and ~50% of the gait cycle, respectively²¹. Measurements of cartilage thickness in the regions of articular contact obtained for an entire gait cycle at multiple joints and across a wide

range of daily activities would allow a more comprehensive evaluation of the effect of mechanical loading on cartilage morphology.

The primary aim of the present study was to measure the locations of articular contact at the TF and PF joints for multiple activities of daily living; specifically, standing, level walking, downhill walking, stair ascent, stair descent, and open-chain (non-weight-bearing) knee flexion. A secondary aim was to investigate the association between the locations of articular contact and cartilage thickness at the TF and PF joints. We hypothesized that thicker cartilage on the femoral condyles, tibial plateaus, femoral trochlea, and patellar facet would be associated with regions of articular contact at both joints in all activities.

MATERIALS AND METHODS

Design: Descriptive cross-sectional study.

Level of Evidence: III.

Participants

Approval for all experimental procedures was granted by the Human Research Ethics Committee at the University of Melbourne. Ten individuals (6M/4F, 29.8±6.1 years, 68.3±9.0 kg, 168.0±9.9 cm) with no knee pain and no history of lower-limb surgery were recruited and gave informed consent.

Computed tomography (CT) and magnetic resonance (MR) imaging

CT scans (Siemens, Munich, Germany; voxel size = 0.35 mm × 0.35 mm × 0.50 mm) and MR scans (3T MRI scanner, Siemens, Munich, Germany; voxel size = 0.625 mm × 0.625 mm × 3.00 mm; proton-density-weighted turbo spin-echo; repetition

time=2000ms; echo time=33ms; flip angle=150°; echo train length=7) of the right knee were obtained with the participant lying supine and the knee extended. The CT and MR scans were segmented using 3D Slicer²² to create geometric models of the bone and articular cartilage surfaces for the femur, tibia and patella. The cartilage models were aligned to the bone models using Geomagic Studio (3D Systems, USA)²³. The surface of each bone and cartilage was defined as a series of triangles with an edge length of ~1 mm.

Cartilage thickness

The thickness of cartilage covering the femur, tibia, and patella was measured for each participant. A line was cast normal to each subchondral bone surface triangle from its center, and the length of the line segment within the cartilage layer was used as a measure of cartilage thickness. Koo et al.²⁴ assessed the accuracy of this method in measuring knee cartilage thickness and reported a mean error of ± 0.3 mm. Because the MR image slice spacing in the present study was twice that used by Koo et al.²⁴ (i.e., 3.0 mm vs 1.5 mm), an additional analysis was performed to estimate the uncertainty in our measurements of cartilage thickness. A single high-resolution MR scan (voxel size = 0.35 mm \times 0.35 mm \times 0.35 mm) was resampled to approximate the MR image slice spacing used in the present study and that adopted by Koo et al.²⁴. Increasing the MR image slice spacing by ~1.5 mm increased the mean error in the measured cartilage thickness by no more than 0.07 mm.

Human motion experiments

Each participant performed six activities: standing, level walking, downhill walking, stair ascent, stair descent, and open-chain (non-weight-bearing) knee flexion. Full-body motion, ground reaction forces (GRFs), and biplane X-ray images were recorded

simultaneously for each activity. Full-body motion data were recorded using a nine-camera motion capture system (VICON, Oxford, UK) operating at 120 Hz. GRFs were measured using three force plates (AMTI, Watertown, MA) sampling at 1080 Hz. Biplane X-ray images of the right knee were captured using a Mobile Biplane X-ray (MoBiX) imaging system ($1,024 \times 1,024$ pixels, 200 frames/sec, 1/200 sec exposure time, 110 kV, 13.1 mA)²⁵. The full-body motion and GRF data were used to identify key events during the gait cycle. Details of the experimental protocol are given in Thomeer et al.²⁶.

Tibiofemoral and patellofemoral kinematics

Six-degree-of-freedom (6-DOF) TF and PF joint kinematics were calculated from pose estimation by combining the geometric bone models and biplane X-ray images. Pose-estimation was performed using custom MATLAB (MathWorks Inc., Natick, MA) software. The resultant joint kinematics were filtered using a fourth-order, low-pass Butterworth filter with a cutoff frequency of 10 Hz. The data for each activity were then resampled to 201 time points at equal intervals each representing 0.5% of the activity. Maximum root-mean-square errors (RMSEs) associated with 6-DOF kinematic measurements obtained for the intact knee were previously reported to be 0.78 mm and 0.77° for translations and rotations of the tibia relative to the femur²⁵ and 0.37 mm and 1.46° for translations and rotations of the patella relative to the femur²⁷.

Location of articular cartilage contact

Articular contact was defined by the intersection of the cartilage layers lining two opposing bones. The location of cartilage contact was determined using a five-step procedure (Fig. 1). First, geometric models of the bones and their corresponding

cartilage models were transformed to their respective positions and orientations in a common reference frame. Second, cartilage models were represented by volumetric point clouds with individual points spaced 0.22 mm apart in a regular 3D grid. Third, points appearing in both cartilage point clouds were used to find the intersection of the two cartilage models, which defined the contact volume. Fourth, the center of the triangle closest to the centroid of the contact volume was identified as the center of cartilage contact. Finally, each point defining the contact volume was mapped to the closest surface triangle to determine the contact region. This process was repeated for all 201 time points at both the TF and PF joints for each activity. The locations of the cartilage contact centers were normalized using the ratio of each participant's femoral bicondylar width to the mean femoral bicondylar width calculated for all 10 participants.

An *in vitro* experiment was performed to evaluate the accuracy with which biplane X-ray imaging and MR imaging could be used to locate knee cartilage contact centers. 6-DOF TF and PF joint kinematics were measured using biplane X-ray imaging as a cadaver limb was actuated to simulate loaded knee flexion²³. The kinematic data were then combined with geometric models of the bones and cartilage surfaces to determine the locations of cartilage contact centers at the TF and PF joints. These contact locations were validated against measurements obtained simultaneously in the same specimen using a pressure sensor (Tekscan 4000, Tekscan, Inc., Boston, MA). RMSEs in the locations of the cartilage contact centers on the medial tibial plateau, lateral tibial plateau, and patellar facet were 1.7 mm, 2.0 mm, and 2.7 mm, respectively. Details of the cadaver experiments are given by Gu and Pandy²³.

Data analysis

Means and peak-to-peak displacements of the cartilage contact centers on the tibia, femur and patella were calculated for each activity. For each dynamic activity (i.e., all activities other than standing), the contact center locations on the tibia, femur and patella averaged across all participants were plotted against the tibiofemoral flexion angle. A cubic spline function was then fitted to the data to calculate a coefficient of determination (r^2) for each contact center trajectory²⁶. A contact center trajectory was assumed to be coupled to the tibiofemoral flexion angle if $r^2 \geq 0.70$, moderately related if $0.50 \leq r^2 < 0.70$, and weakly related if $r^2 < 0.50$.

A one-way analysis of variance (ANOVA) with Tukey's post-hoc test was used to determine significant differences in cartilage thickness across seven zones at the knee: medial tibial plateau, lateral tibial plateau, medial femoral condyle, lateral femoral condyle, entire femoral cartilage, femoral trochlea, and patellar facet.

Significant differences in the thicknesses of contacting and non-contacting cartilage were tested using two-tailed paired t-tests. Tests were conducted for each of the four zones at the TF joint: medial and lateral tibial and femoral cartilages; for each of the two zones at the PF joint: patellar and femoral cartilages; and for all six of the aforementioned TF and PF zones pooled together. Surface triangles within a cartilage zone were defined as contacting or non-contacting separately for each activity. For any knee cartilage zone (e.g., medial tibial plateau) during each activity, a surface triangle was defined as contacting if it came into contact with knee cartilage from another zone (e.g., medial femoral condyle) for at least one time point during that activity. Conversely, a surface triangle was defined as non-contacting if it did not come into contact with cartilage from any other knee cartilage zone at any point

during that activity. For each knee cartilage zone, the regions of contacting and non-contacting cartilage were found by summing up all the contacting and non-contacting surface triangles, respectively. The region of contacting cartilage was calculated for one full cycle of each activity rather than at discrete time points only when the knee was weightbearing because joint contact forces can be transmitted by the knee during both the weightbearing (stance) and non-weightbearing (swing) phases of the gait cycle²⁸. For example, the peak force transmitted by the PF joint during normal walking occurs during the swing phase when the knee is highly flexed²¹. A Bonferroni correction for multiple comparisons was applied when interpreting the results of the two-tailed paired t-tests, where the initial threshold was divided by the number of comparisons to obtain the significance threshold. Specifically, 42 comparisons were performed for 7 cartilage zones across 5 activities with all activities pooled, resulting in a Bonferroni correction of $0.05 / 42 = 0.001$.

RESULTS

Cartilage thickness

Cartilage was thickest on the patella and femoral trochlea and thinnest on the femoral condyles and medial tibial plateau (Fig. 2). Patellar cartilage was thickest on the lateral facet in the region roughly midway between the inferior and superior borders of the articular surface (Fig. 2A). The mean thickness of the patellar cartilage was 3.1 mm and peak thickness ranged from 4.7 mm to 6.0 mm (Fig. 2B). Femoral cartilage was thickest on the superior portion of the trochlear groove, with peak thickness in this region ranging from 4.1 mm to 5.8 mm. Cartilage covering the medial and lateral femoral condyles was approximately the same thickness (mean = 2.3 mm; peak = 3.8 mm). Cartilage covering the lateral tibial plateau (peak thickness: 4.0 to 5.4 mm) was

thicker than that on the medial tibial plateau (peak thickness: 3.4 to 4.4 mm). Tibial cartilage was thickest in the regions bordering the medial and lateral intercondylar eminences.

Paths of the cartilage contact centers

The contact centers traced remarkably similar paths on the femur and patella across all activities while their locations on the tibia were more varied (Figs. 3-6, panel A). There were marked differences in the time histories of the contact centers between activities (Figs. 3-6, panel B, columns 1-3), but most of these trajectories coalesced when the data were plotted against the TF flexion angle (Figs. 3-6, panel B, column 4). This was particularly evident in the paths of the contact centers measured on the femoral condyles, trochlear groove, and patella (Figs. 4-6, panel B, column 4). In contrast, the paths of the contact centers on the tibial plateau were markedly different between activities, even when the data were represented as a function of the TF flexion angle. For example, the contact center was located more anteriorly on the lateral tibial plateau in open-chain flexion than in any of the ambulatory activities, particularly as TF flexion increased beyond 50° (Fig. 3B, row 3, column 4). In standing, the contact centers on the lateral tibial plateau and medial and lateral femoral condyles were located more anteriorly compared to those measured during any of the dynamic activities (Figs. 3-4).

Across all activities, mean peak-to-peak anterior-posterior displacement of the TF contact center was significantly greater on the medial tibial plateau (10.3 ± 0.9 mm) than the lateral tibial plateau (6.9 ± 0.9 mm) ($p=0.003$) (Fig. 3). Mean peak-to-peak anterior-posterior displacement of the TF contact center was also significantly greater on the medial femoral condyle (29.4 ± 1.7 mm) than the lateral femoral condyle

(21.7±1.0 mm) ($p<0.001$) (Fig. 4). The contact centers followed a conspicuously narrow path along the medial and lateral femoral condyles and deviated minimally in the medial-lateral direction during all activities (Fig. 4). The paths of the contact centers on the femoral condyles were perfectly coupled to the TF flexion angle in the superior-inferior and anterior-posterior directions ($r^2=1.00$). Contact-center paths on the tibia in the anterior-posterior direction were coupled to the TF flexion angle on the medial plateau ($r^2=0.92$) but only moderately related to the flexion angle on the lateral plateau ($r^2=0.62$).

The contact centers on the patella and femoral trochlea translated mainly in the superior-inferior direction (Figs. 5-6). In all activities, the contact center on the patella was located slightly lateral to the ridge dividing the medial and lateral facets while that on the femur was confined to the lateral surface of the trochlear groove. During open-chain flexion, the locations of the contact centers on the patella and femoral trochlea deviated sharply in the lateral direction when the knee was bent beyond 90°. The paths of the contact centers on the patella and femoral trochlea were coupled to the TF flexion angle in all activities ($r^2 \geq 0.80$) (Figs. 5-6, panel B, column 4).

Association between cartilage contact and cartilage thickness

The regions of contacting cartilage were significantly thicker than the regions of non-contacting cartilage on the patella, femoral trochlea, medial tibial plateau, and lateral tibial plateau in all activities ($p<0.001$) (Fig. 7). There were no significant differences in thickness between contacting and non-contacting cartilage on the medial femoral condyle in all activities ($p>0.02$). There were also no significant differences in thickness between contacting and non-contacting cartilage on the lateral femoral condyle in all activities, except open-chain knee flexion ($p<0.001$). The differences in

thickness between contacting and non-contacting cartilage were similar in magnitude for the patella, femoral trochlea, medial tibial plateau, and lateral tibial plateau, where the regions of contacting cartilage were on average 0.9 mm, 0.8 mm, 0.9 mm, and 1.0 mm thicker than the regions of non-contacting cartilage, respectively.

DISCUSSION

We measured the locations of cartilage contact in the healthy knee during six functional activities and determined the association between the regions of contacting cartilage and cartilage thickness on the medial and lateral tibial plateaus, medial and lateral femoral condyles, femoral trochlea, and patellar facet. The contact centers traced similar paths on the medial and lateral femoral condyles, femoral trochlea, and patellar facet in all activities while their locations on the tibial plateau were more varied between activities. Contacting cartilage was significantly thicker than non-contacting cartilage on the patella, femoral trochlea, medial tibial plateau and lateral tibial plateau in all activities ($p < 0.001$). There were no significant differences in thickness between contacting and non-contacting cartilage on the medial and lateral femoral condyles in all activities other than open-chain knee flexion, thus our hypothesis regarding the association between cartilage contact and cartilage thickness was only partially supported.

Our measurements of knee cartilage thickness compare favorably with data reported by others²⁹⁻³¹. Eckstein et al.³¹ measured cartilage thickness on the patella, femoral trochlea, femoral condyles, and tibial plateau in 27 healthy individuals aged 23 to 64 years. They found that cartilage was thickest on the patella and that the mean thickness of patellar cartilage was significantly greater than that covering the femoral trochlea, femoral condyles and tibial plateau. Eckstein et al.³¹ also found mean

cartilage thickness on the femoral trochlea and lateral tibial plateau to be greater than that on the medial tibial plateau and either of the femoral condyles. Our data are in broad agreement with these findings (Fig. 2).

Our measurements of the locations of cartilage contact in the PF compartment are also consistent with results reported by others^{13,32}. In a study of 12 healthy individuals performing a step-up maneuver, Suzuki et al.³³ found the PF contact center to lie slightly lateral to the vertical ridge on the patella and slightly lateral to the center of the trochlear groove on the femur. The results of cadaver studies also indicate that PF contact is confined mainly to the lateral compartment, with approximately two-thirds of the contact force transmitted by the lateral patellar facet during knee extension³². In the present study, the PF contact center was concentrated in the lateral compartment during all six activities (Figs. 5 and 6).

There are notable differences between our measurements of the locations of cartilage contact on the tibia and corresponding data in the literature. Li et al.¹¹ found that anterior-posterior translation of the cartilage contact center was greater on the lateral tibial plateau than the medial tibial plateau whereas our data show the opposite trend (Fig. 3). Our findings are more consistent with those of Liu et al.⁸ who reported that anterior-posterior translation of the TF contact center on the medial tibial plateau was greater than that on the lateral tibial plateau during the stance phase of gait. These differences in the measured locations of the centers of cartilage contact may be explained by the different activities studied: our measurements and those of Liu et al.⁸ apply to dynamic movements whereas Li et al.¹¹ recorded data for a static single-leg lunge. We note here that the accuracy of our measurements of knee cartilage contact is comparable to that reported by others. Thorhauer and Tashman³⁴ performed a series

of cadaver experiments to measure the locations of cartilage contact on the tibial plateau using biplane X-ray imaging and cartilage models created from both MRI scans and a gold-standard laser scanning technique. They reported RMSEs of 1.8 mm and 2.1 mm for the medial and lateral tibial plateau, respectively, which are closely similar to the RMSEs obtained from our own cadaver experiments (i.e., 1.7 mm and 2.0 mm for the medial and lateral tibial plateau as noted in the Methods section above).

Our results suggest that the paths of TF and PF contact on the femur and patella are determined mainly by knee-joint geometry rather than muscle loading, which would have varied considerably across the activities examined here^{35,36}. The contact forces transmitted by the PF joint in stair ascent and stair descent are much higher than that associated with level walking³⁷, yet the paths of the contact centers on the femoral trochlea and patellar facet in these three activities were surprisingly similar. In addition, the TF contact center was located on the lateral third of the medial femoral condyle and on the central third of the lateral femoral condyle in all activities (Fig. 4A), while the translations of the TF contact center on the femur were perfectly coupled to the TF flexion angle in both the superior-inferior and anterior-posterior directions (Fig. 4, column 4: $r^2=1.00$ for both). These results indicate that the paths of the PF contact center on the trochlear groove and patellar facet and those of the TF contact center on the femoral condyles are independent of the type of activity performed and are determined instead by the shapes of the articulating surfaces of the bones and the lines of action of the muscles and ligaments crossing the knee.

Our findings offer only partial support for the proposition that cartilage morphology is adapted to joint load^{1,2,4,14}. In all activities, the regions of contacting cartilage

coincided with thicker cartilage on the patella, tibia and femoral trochlea but not so on the femoral condyles (Fig. 7). Liu et al.⁸ also found that articular contact at the TF joint corresponds with regions of thicker cartilage covering the tibia but not the femur. Koo et al.¹⁹ and Scanlan et al.²⁰ reported a significant positive relationship between cartilage contact and cartilage thickness on the femoral condyles for level walking, although these authors compared the location of cartilage contact and cartilage thickness at a single time point (heel-strike) whereas our analysis extends over the entire gait cycle. Li et al.¹¹ found that the centers of cartilage contact at the TF joint coincided with thicker cartilage on the medial and lateral femoral condyles and on the medial and lateral tibial plateaus for a single-leg lunge. Eckstein et al.¹⁸ measured mean cartilage thickness on the articulating surfaces of the patella, femoral trochlea, medial and lateral tibial plateaus, and medial and lateral femoral condyles in well-trained triathletes and inactive controls and found no difference between these two groups. They concluded that cartilage morphology may not be adapted to joint load and suggested instead that lower cartilage stresses may be facilitated by the larger joint surface areas evident in the knees of the triathletes.

Simon et al.³⁸ and Shepherd and Seedhom³⁹ proposed that joint congruence rather than joint load may explain differences in cartilage thickness observed at the weight-bearing joints. Incongruent joints, such as the knee, are covered by relatively thick cartilage whereas congruent joints, such as the ankle, have a thin covering of articular cartilage. Compressive stress is reduced at an incongruent joint because as the thick cartilage layer deforms the contact area increases. In contrast, congruent joints reduce stress by spreading the load over the larger contact area produced by the congruency of the mating bone surfaces. Measurements of joint surface topography and cartilage thickness in the regions of articular contact together with estimates of joint stress are

needed to evaluate the relative influence of mechanical load and joint congruence on cartilage morphology.

Based on biplane X-ray imaging measurements of 6-DOF knee kinematics obtained from the same participants performing the same activities investigated in the current study, we previously reported that the center of the lateral femoral condyle translates further on the tibial plateau than the center of the medial femoral condyle^{26,40}. Consistent with the movements of the condylar centers, the center of rotation of the knee in the transverse plane was located in the medial compartment of the TF joint^{26,40}. In the present study we found that peak-to-peak anterior-posterior displacement of the contact center on the medial tibial plateau was ~3.5 mm greater than that on the lateral tibial plateau (Fig. 3). This, however, does not imply that the center of rotation of the knee in the transverse plane resides in the lateral TF compartment. Caution is advised when using the paths traced by the cartilage contact centers on the tibial plateau to infer the location of the transverse center of rotation of the knee. Whilst the displacements of the femoral condylar centers may accurately reflect the location of the center of rotation in the transverse plane, they cannot be used to deduce the locations of the cartilage contact centers on the tibial plateau. As illustrated in Figure 8, the displacements of the contact centers on the medial and lateral tibial plateaus are governed by the shapes of the tibial articular surfaces³. Because the medial tibial plateau is concave and the lateral tibial plateau convex, equivalent anterior-posterior displacements of the centers of the medial and lateral femoral condyles would result in the contact center translating further on the medial tibial plateau than the lateral tibial plateau. This explains why it is possible for peak-to-peak anterior-posterior displacements of the contact center on the medial tibial plateau to be greater than those on the lateral tibial plateau (Fig. 3), even though the

center of the lateral femoral condyle translated further than the center of the medial femoral condyle in all activities²⁶. Other factors such as the medial femoral condyle being larger than the lateral femoral condyle and the presence of a mobile meniscus further highlight that caution is needed when inferring the locations of the cartilage contact centers on the tibial plateau from the translations of the centers of the femoral condyles.

One limitation of the present study is that regions of articular cartilage contact were used to deduce the presence of joint contact load at the knee. Because the magnitude of joint contact force cannot be measured non-invasively *in vivo*, we implicitly assumed that for any given activity contacting cartilage experienced higher joint forces than non-contacting cartilage, an assumption commonly invoked in previous studies examining the association between articular cartilage contact and cartilage thickness^{8,11,19,20}. The adduction moment is often used as a surrogate measure of the contact force acting at the knee during gait⁴¹. It has been shown that thicker cartilage covering the medial femoral condyle correlates with a higher knee adduction moment in normal walking^{1,42}, implying that cartilage structurally adapts to the magnitude of joint load. Future studies should focus on deriving accurate estimates of the time histories of TF and PF joint contact forces during daily activities to test for associations between the magnitude of joint contact force and cartilage thickness. A second limitation is that the menisci cannot be visualized on the X-ray images, hence the relative movements of the menisci and bones could not be taken into account when determining the center of cartilage contact at the TF joint. In our analysis, articular cartilage on any given bone that did not come into contact with articular cartilage on an opposing bone was defined as non-contacting (i.e., only cartilage-to-cartilage contact was considered). While this was an accurate assumption for the

patella and femoral trochlea, some of the cartilage defined as non-contacting on the tibial plateau and femoral condyles could have come into contact with the menisci. This limitation may explain why our results show a stronger association between cartilage contact location and cartilage thickness at the PF joint than the TF joint. Finally, participants in the current study were not instructed to minimize their weightbearing activity prior to the MR scans, and so knee cartilage thickness may have been less than in the resting state. However, the magnitude of total cartilage thinning resulting from fluid exudation and tissue consolidation during weightbearing activity has been found to be relatively small. For example, Kersting et al.⁴³ found a 3% decrease in knee cartilage volume following 1 hour of weightbearing exercise. In any event this limitation is unlikely to alter our results for the association between cartilage contact and cartilage thickness because we measured cartilage contact while the knee was loaded during dynamic activity. In addition, our measurements of knee cartilage thickness are consistent with data reported previously by others²⁹⁻³¹ as noted above.

In summary, we quantified the locations of cartilage contact at the TF and PF joints for a wide range of daily activities. Our results provide partial support for the proposition that cartilage morphology (thickness) is adapted to joint load and leave open the possibility that other factors like joint congruence³⁸ also play a role in regulating the structure of healthy cartilage. The data may be used as a guide when evaluating articular contact in osteoarthritic and reconstructed knees.

ACKNOWLEDGEMENTS

This work was supported in part by a Discovery Projects grant (DP120101973) from the Australian Research Council. LTT was supported in part by a Postgraduate Scholarship provided by the University of Melbourne.

References

1. Andriacchi TP, Koo S, Scanlan SF. 2009. Gait mechanics influence healthy cartilage morphology and osteoarthritis of the knee. *The Journal of Bone and Joint Surgery American Volume* 91:95.
2. Carter DR, Beaupre GS, Wong M, et al. 2004. The mechanobiology of articular cartilage development and degeneration. *Clinical Orthopaedics and Related Research*:69-77.
3. Andriacchi TP, Briant PL, Bevill SL, et al. 2006. Rotational changes at the knee after ACL injury cause cartilage thinning. *Clinical Orthopaedics and Related Research* 442:39-44.
4. Seedhom B. 2006. Conditioning of cartilage during normal activities is an important factor in the development of osteoarthritis. *Rheumatology* 45:146-149.
5. Stergiou N, Ristanis S, Moraiti C, et al. 2007. Tibial rotation in anterior cruciate ligament (ACL)-deficient and ACL-reconstructed knees. *Sports Medicine* 37:601-613.
6. Elias JJ, Kilambi S, Goerke DR, et al. 2009. Improving vastus medialis obliquus function reduces pressure applied to lateral patellofemoral cartilage. *Journal of Orthopaedic Research* 27:578-583.
7. Bingham J, Papannagari R, Van de Velde S, et al. 2008. In vivo cartilage contact deformation in the healthy human tibiofemoral joint. *Rheumatology* 47:1622-1627.
8. Liu F, Kozanek M, Hosseini A, et al. 2010. In vivo tibiofemoral cartilage deformation during the stance phase of gait. *Journal of Biomechanics* 43:658-665.
9. Hosseini A, Van de Velde S, Gill TJ, et al. 2012. Tibiofemoral cartilage contact biomechanics in patients after reconstruction of a ruptured anterior cruciate ligament. *Journal of Orthopaedic Research* 30:1781-1788.

10. Van de Velde SK, Bingham JT, Hosseini A, et al. 2009. Increased tibiofemoral cartilage contact deformation in patients with anterior cruciate ligament deficiency. *Arthritis & Rheumatism* 60:3693-3702.
11. Li G, Park SE, DeFrate LE, et al. 2005. The cartilage thickness distribution in the tibiofemoral joint and its correlation with cartilage-to-cartilage contact. *Clinical Biomechanics* 20:736-744.
12. Akpınar B, Thorhauer E, Tashman S, et al. 2019. Tibiofemoral cartilage contact differences between level walking and downhill running. *Orthopaedic Journal of Sports Medicine* 7:2325967119836164.
13. Suzuki T, Hosseini A, Li JS, et al. 2012. In vivo patellar tracking and patellofemoral cartilage contacts during dynamic stair ascending. *Journal of Biomechanics* 45:2432-2437.
14. Chaudhari AM, Briant PL, Bevill SL, et al. 2008. Knee kinematics, cartilage morphology, and osteoarthritis after ACL injury. *Medicine and Science in Sports and Exercise* 40:215-222.
15. Jones G, Ding C, Glisson M, et al. 2003. Knee articular cartilage development in children: a longitudinal study of the effect of sex, growth, body composition, and physical activity. *Pediatric Research* 54:230-236.
16. Kiviranta I, Tammi M, Jurvelin J, et al. 1988. Moderate running exercise augments glycosaminoglycans and thickness of articular cartilage in the knee joint of young beagle dogs. *Journal of Orthopaedic Research* 6:188-195.
17. Vanwanseele B, Eckstein F, Knecht H, et al. 2003. Longitudinal analysis of cartilage atrophy in the knees of patients with spinal cord injury. *Arthritis & Rheumatism: Official Journal of the American College of Rheumatology* 48:3377-3381.
18. Eckstein F, Faber S, Mühlbauer R, et al. 2002. Functional adaptation of human joints to mechanical stimuli. *Osteoarthritis and Cartilage* 10:44-50.
19. Koo S, Rylander JH, Andriacchi TP. 2011. Knee joint kinematics during walking influences the spatial cartilage thickness distribution in the knee. *Journal of Biomechanics* 44:1405-1409.
20. Scanlan SF, Favre J, Andriacchi TP. 2013. The relationship between peak knee extension at heel-strike of walking and the location of thickest femoral cartilage in ACL reconstructed and healthy contralateral knees. *Journal of Biomechanics* 46:849-854.
21. Thomeer L, Lin Y-C, Pandy M. 2020. Load distribution at the patellofemoral joint during walking. *Annals of Biomedical Engineering* 48:2821-2835.

22. Pieper S, Lorensen B, Schroeder W, et al. 2006. The NA-MIC kit: ITK, VTK, pipelines, grids and 3D slicer as an open platform for the medical image computing community. *Biomedical Imaging: Nano to Macro, 2006 3rd IEEE International Symposium* 698-701.
23. Gu W, Pandy MG. 2020. Direct validation of human knee-joint contact mechanics derived from subject-specific finite-element models of the tibiofemoral and patellofemoral joints. *Journal of Biomechanical Engineering* 142:071001.
24. Koo S, Gold GE, Andriacchi TP. 2005. Considerations in measuring cartilage thickness using MRI: factors influencing reproducibility and accuracy. *Osteoarthritis Cartilage* 13:782-789.
25. Guan S, Gray HA, Keynejad F, et al. 2016. Mobile biplane X-ray imaging system for measuring 3D dynamic joint motion during overground gait. *IEEE Transactions on Medical Imaging* 35:326-336.
26. Thomeer L, Guan S, Gray H, et al. 2020. Six-degree-of-freedom tibiofemoral and patellofemoral joint motion during activities of daily living. *Annals of Biomedical Engineering* 49:1183-1198.
27. Gray HA, Guan S, Pandy MG. 2017. Accuracy of mobile biplane X-ray imaging in measuring 6-degree-of-freedom patellofemoral kinematics during overground gait. *Journal of Biomechanics* 57:152-156.
28. Shelburne KB, Torry MR, Pandy MG. 2005. Muscle, ligament, and joint-contact forces at the knee during walking. *Medicine and Science in Sports and Exercise* 37:1948-1956.
29. Ateshian GA, Soslowsky LJ, Mow VC. 1991. Quantitation of articular surface topography and cartilage thickness in knee joints using stereophotogrammetry. *Journal of Biomechanics* 24:761-776.
30. Cohen ZA, McCarthy DM, Kwak SD, et al. 1999. Knee cartilage topography, thickness, and contact areas from MRI: in-vitro calibration and in-vivo measurements. *Osteoarthritis Cartilage* 7:95-109.
31. Eckstein F, Winzheimer M, Hohe J, et al. 2001. Interindividual variability and correlation among morphological parameters of knee joint cartilage plates: analysis with three-dimensional MR imaging. *Osteoarthritis and Cartilage* 9:101-111.
32. Elias JJ, Kirkpatrick MS, Saranathan A, et al. 2011. Hamstrings loading contributes to lateral patellofemoral malalignment and elevated cartilage pressures: an in vitro study. *Clinical Biomechanics* 26:841-846.

33. Suzuki T, Hosseini A, Li JS, et al. 2012. In vivo patellar tracking and patellofemoral cartilage contacts during dynamic stair ascending. *Journal of Biomechanics* 45:2432-2437.
34. Thorhauer E, Tashman S. 2015. Validation of a method for combining biplanar radiography and magnetic resonance imaging to estimate knee cartilage contact. *Medical Engineering and Physics* 37:937-947.
35. Lin Y-C, Fok LA, Schache AG, et al. 2015. Muscle coordination of support, progression and balance during stair ambulation. *Journal of Biomechanics* 48:340-347.
36. Bergmann G, Bender A, Graichen F, et al. 2014. Standardized loads acting in knee implants. *Plos One* 9:e86035.
37. Chen Y-J, Powers CM. 2014. Comparison of three-dimensional patellofemoral joint reaction forces in persons with and without patellofemoral pain. *Journal of Applied Biomechanics* 30:493-500.
38. Simon WH, FriedenberG S, Richardson S. 1973. Joint congruence: A correlation of joint congruence and thickness of articular cartilage in dogs. *Journal of Bone and Joint Surgery* 55:1614-1620.
39. Shepherd D, Seedhom B. 1999. Thickness of human articular cartilage in joints of the lower limb. *Annals of the Rheumatic Diseases* 58:27-34.
40. Gray HA, Guan S, Thomeer LT, et al. 2019. Three-dimensional motion of the knee-joint complex during normal walking revealed by mobile biplane x-ray imaging. *Journal of Orthopaedic Research* 37:615-630.
41. Schipplein O, Andriacchi T. 1991. Interaction between active and passive knee stabilizers during level walking. *Journal of Orthopaedic Research* 9:113-119.
42. Andriacchi TP, Mündermann A, Smith RL, et al. 2004. A framework for the in vivo pathomechanics of osteoarthritis at the knee. *Annals of Biomedical Engineering* 32:447-457.
43. Kersting UG, Stubendorff JJ, Schmidt MC, et al. 2005. Changes in knee cartilage volume and serum COMP concentration after running exercise. *Osteoarthritis and Cartilage* 13:925-934.

FIGURE CAPTIONS

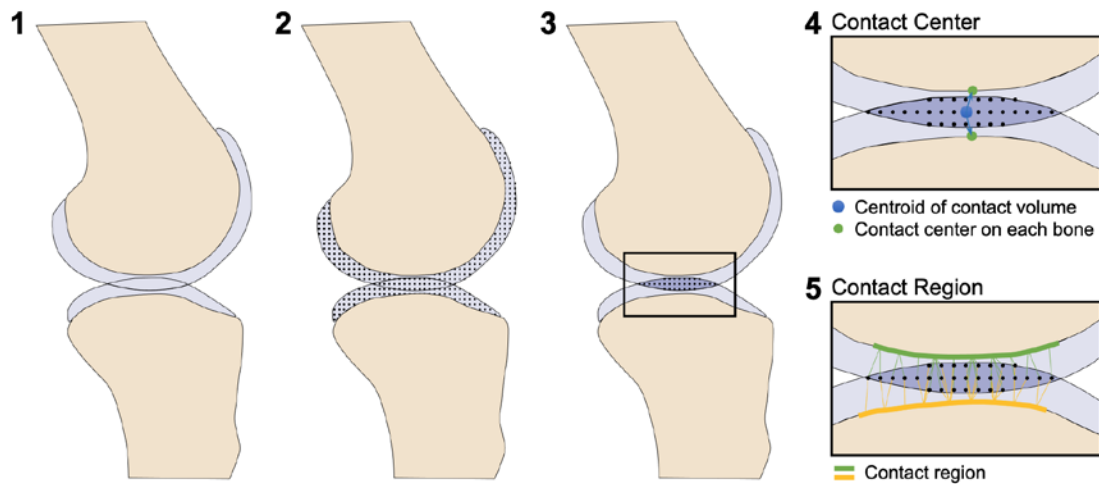


Fig. 1: Two-dimensional schematic diagram illustrating the five-step procedure used to calculate the contact center and contact area at each time point during an activity. Geometric models of each bone and its corresponding layer of articular cartilage were transformed into their respective poses (1) and the cartilage models were replaced with a dense 3D cloud of evenly spaced points (2). The contact volume was defined by the set of coincident points formed by the intersection of the two cartilage point clouds (3). The centroid of the contact volume (blue dot) was mapped to the closest triangle center on each bone surface (green dots) to determine the contact center location (4). Each point in the contact volume was mapped to the closest triangle center on the bone surface to determine the contact region on each bone (green and yellow areas) (5).

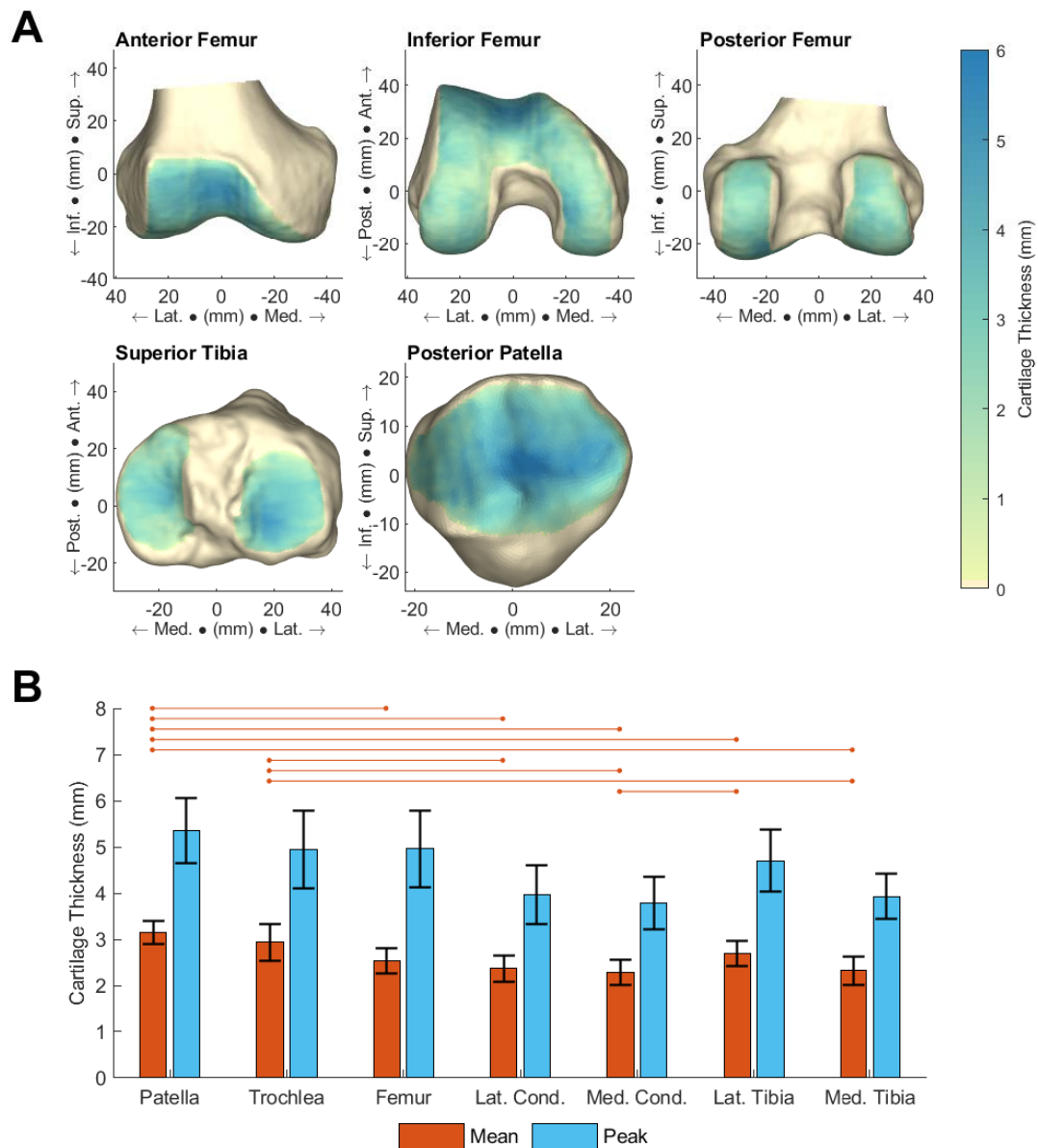


Fig. 2: Articular cartilage thickness on the femur, tibia and patella. (A) Cartilage thickness maps for a single representative participant. (B) Mean and peak cartilage thicknesses measured for all ten participants on the patella, femoral trochlea, femur (all articular cartilage covering the femur), lateral femoral condyle, medial femoral condyle, lateral tibial plateau and medial tibial plateau. Error bars indicate ± 1 standard deviation. The red horizontal lines indicate significant differences between mean cartilage thicknesses. Sup. –

superior, Inf. – inferior, Ant. – anterior, Post. – posterior, Lat. – lateral, Med. – medial, Cond. – condyle.

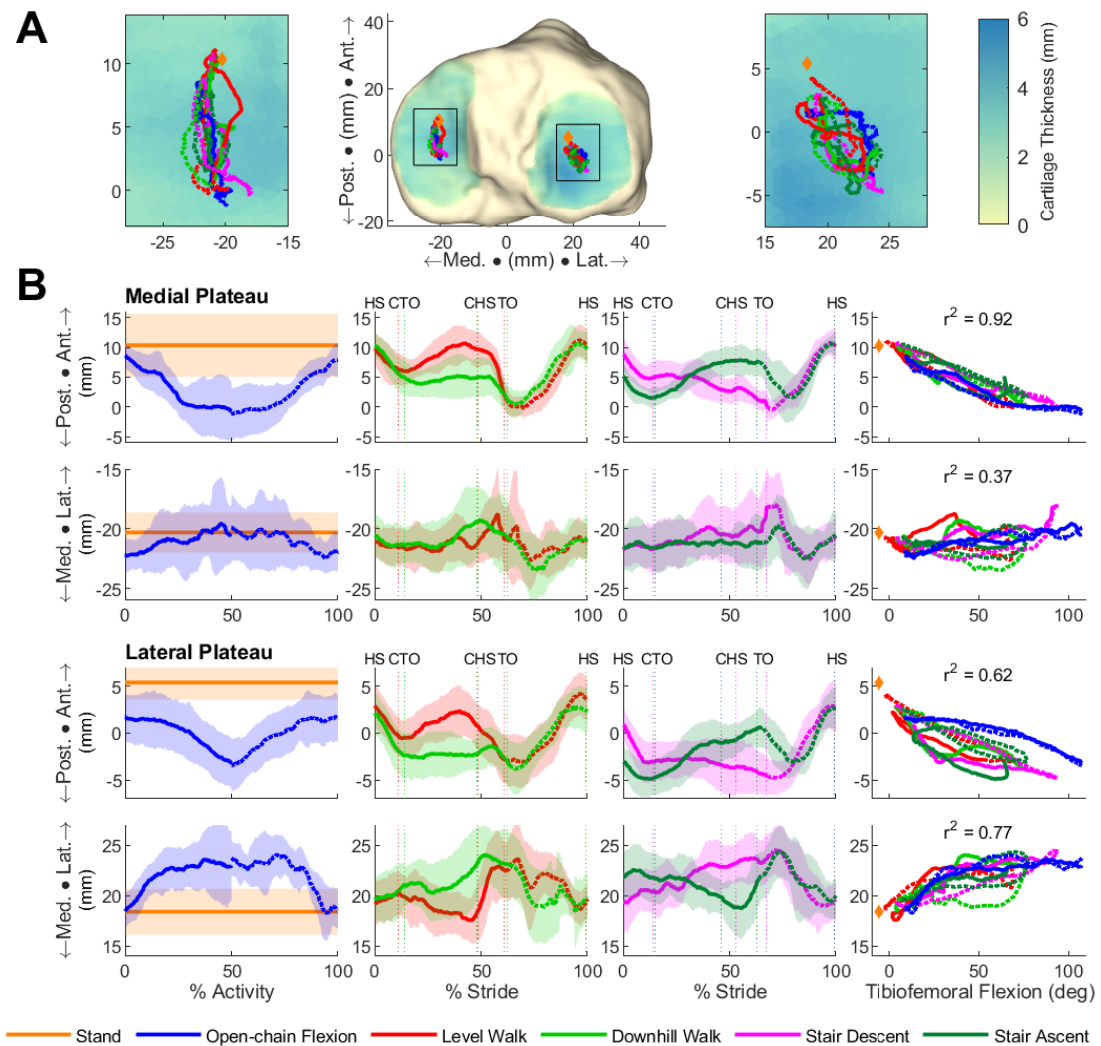


Fig. 3: Locations of the tibiofemoral cartilage contact centers measured on the tibia for the six activities studied. (A) Locations of the mean tibial cartilage contact centers are projected onto the tibial plateaus of a right knee and viewed superiorly. The bone and cartilage models are from a single representative participant. (B) Locations of the medial and lateral mean tibial cartilage contact centers are plotted against percentage of activity duration in columns 1-3 and against the tibiofemoral flexion angle in column 4. The

displacements of the contact centers in the superior-inferior direction were small (peak-to-peak displacement=2.29 mm) and are therefore not shown here. r^2 values indicate the degree of coupling between the path of each contact center and the tibiofemoral flexion angle. Each shaded region represents ± 1 standard deviation from the mean. For open-chain flexion the solid and dotted lines represent the flexion and extension phases, respectively. For each ambulatory activity the solid and dotted lines represent the stance and swing phases, respectively. Key gait events are marked with dotted vertical lines and indicate HS (heel-strike), TO (toe-off), CHS (contralateral heel-strike) and CTO (contralateral toe-off).

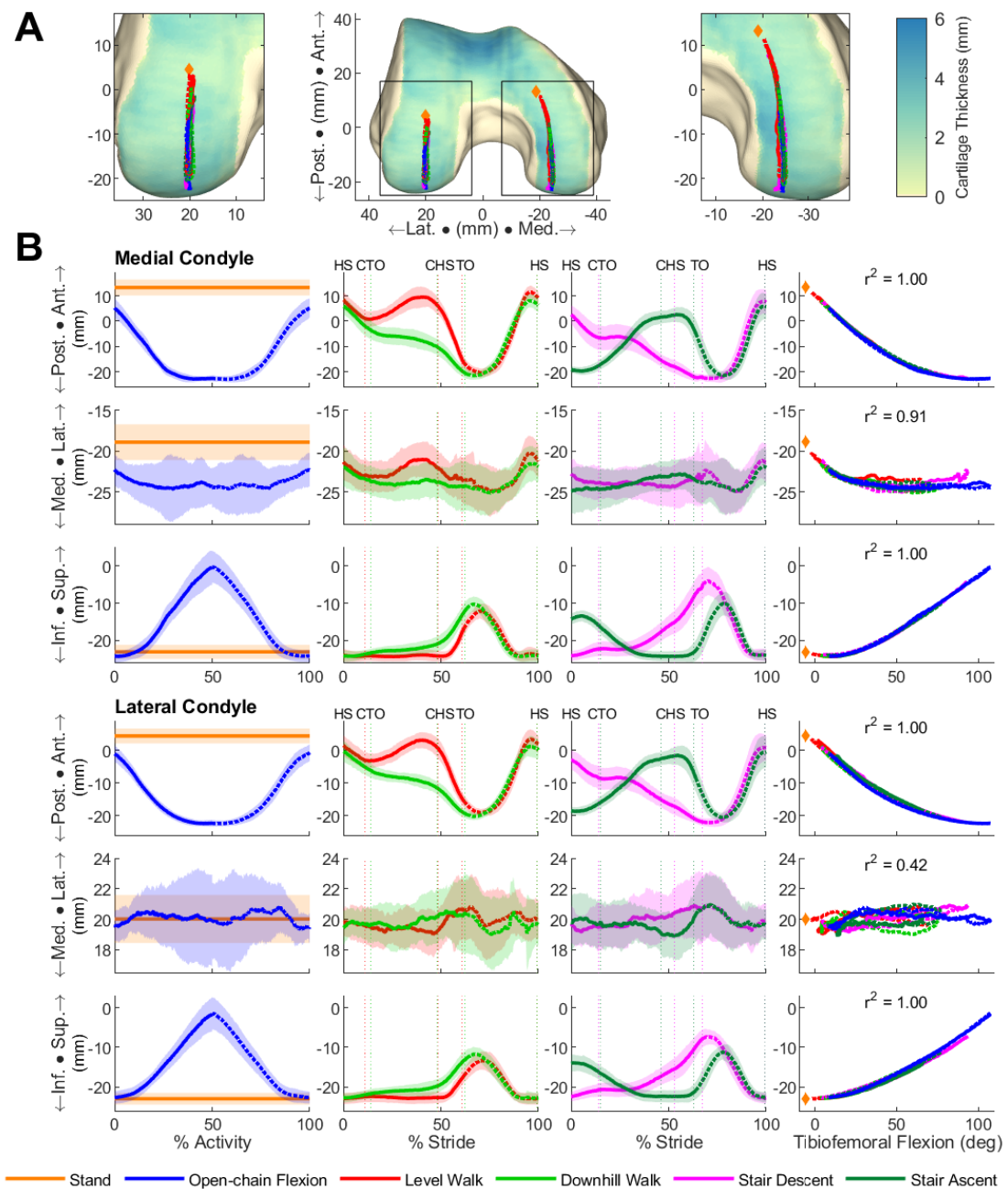


Fig. 4: Locations of the tibiofemoral cartilage contact centers measured on the femur for the six activities studied. (A) Locations of the mean tibiofemoral cartilage contact centers are projected onto the femoral condyles of a right knee and viewed inferiorly. The bone and cartilage models are from a single representative participant. (B) Locations of the medial and lateral mean tibiofemoral cartilage contact centers on the femur are plotted against percentage of activity duration in columns 1-3 and against tibiofemoral

flexion angle in column 4. r^2 values indicate the degree of coupling between the path of each contact center and the tibiofemoral flexion angle. Each shaded region represents ± 1 standard deviation from the mean. For open-chain flexion the solid and dotted lines represent the flexion and extension phases, respectively. For each ambulatory activity the solid and dotted lines represent the stance and swing phases, respectively. Key gait events are marked with dotted vertical lines and indicate HS (heel-strike), TO (toe-off), CHS (contralateral heel-strike) and CTO (contralateral toe-off).

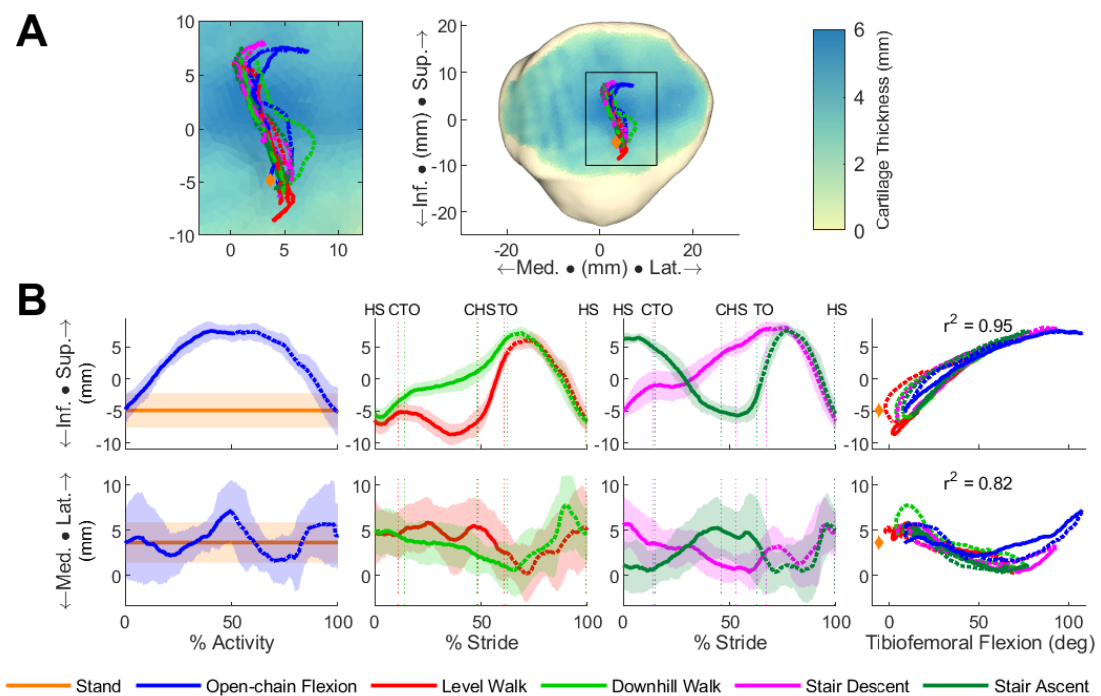


Fig. 5: Locations of the patellofemoral cartilage contact centers measured on the patellar facet for the six activities studied. (A) Locations of the mean patellar cartilage contact centers are projected onto the posterior surface of a right patella. The bone and cartilage models are from a single representative participant. (B) Locations of the mean cartilage contact centers on the patella are plotted against percentage of activity duration in columns 1-3 and against

the tibiofemoral flexion angle in column 4. The displacements of the contact centers in the anterior-posterior direction were small (peak-to-peak displacement=3.73 mm) and are therefore not shown. r^2 values indicate the degree of coupling between the path of each contact center and the tibiofemoral flexion angle. Each shaded region represents ± 1 standard deviation from the mean. For open-chain flexion the solid and dotted lines represent the flexion and extension phases, respectively. For each ambulatory activity the solid and dotted lines represent the stance and swing phases, respectively. Key gait events are marked with dotted vertical lines and indicate HS (heel-strike), TO (toe-off), CHS (contralateral heel-strike) and CTO (contralateral toe-off).

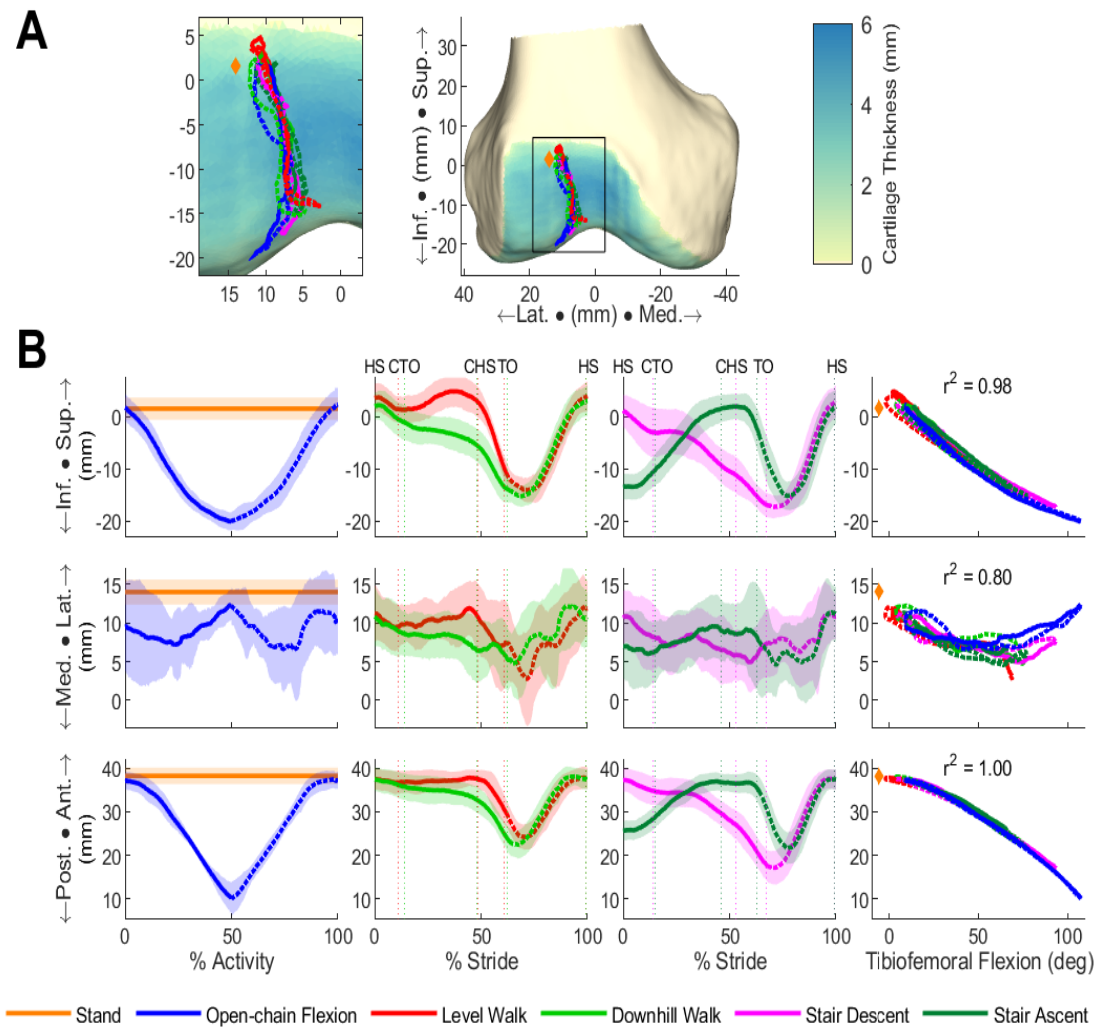


Fig. 6: Locations of the patellofemoral cartilage contact centers measured on the femur for the six activities studied. (A) Locations of the mean femoral cartilage contact centers are projected onto the anterior surface of the femur of a right knee. The bone and cartilage models are from a single representative participant. (B) Locations of the mean femoral cartilage contact centers are plotted against percentage of activity duration in columns 1-3 and against the tibiofemoral flexion angle in column 4. r^2 values indicate the degree of coupling between the path of each contact center and the tibiofemoral flexion angle. Each shaded region represents ± 1 standard deviation from the mean. For open-chain flexion the solid and dotted lines

represent the flexion and extension phases, respectively. For each ambulatory activity the solid and dotted lines represent the stance and swing phases, respectively. Key gait events are marked with dotted vertical lines and indicate HS (heel-strike), TO (toe-off), CHS (contralateral heel-strike) and CTO (contralateral toe-off).

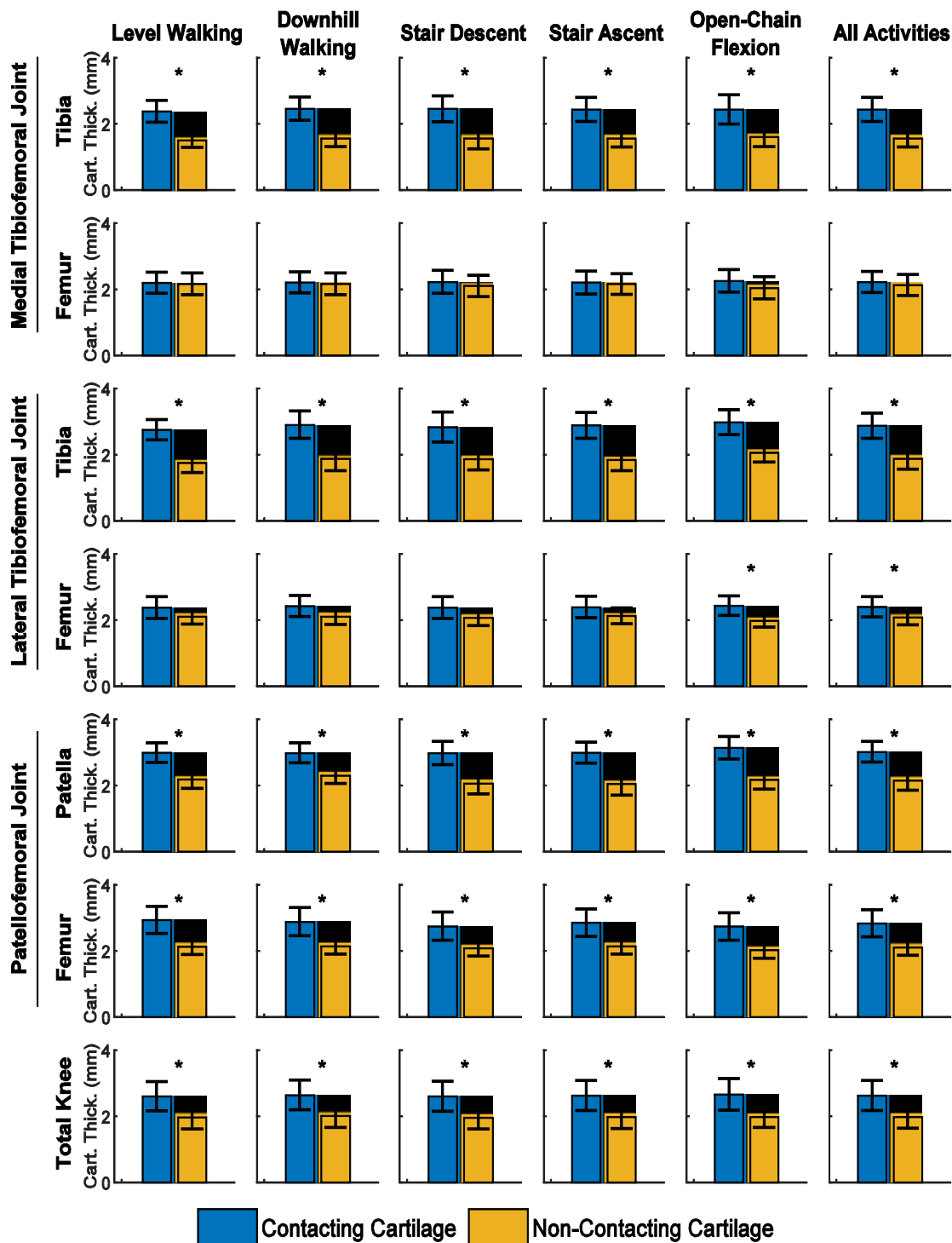


Fig. 7: Thicknesses of contacting and non-contacting cartilage compared across the different cartilage zones and activities. The analysis was performed for all the dynamic activities only, thus data for standing are not shown. Each of the first six rows presents data for one of the six cartilage zones whereas the last

row pools the data from all six zones. Similarly, each of the first five columns presents data for a single activity while the last column pools the data from all activities. The asterisk (*) indicates that a statistically significant difference between the thicknesses of contacting and non-contacting cartilage was found using a two-tailed paired t-test. A threshold of $p=0.001$ was used to identify statistical significance based on a Bonferroni correction with an initial threshold of 0.05 and 42 comparisons (see text).

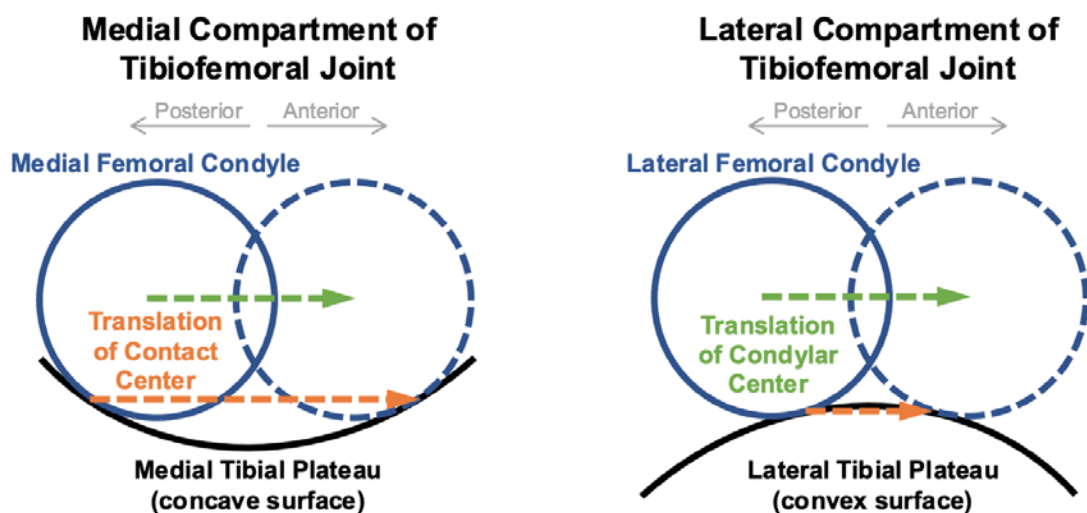


Fig. 8: Diagram illustrating that larger translations of the femoral condylar center do not necessitate larger translations of the tibiofemoral contact center on the tibial plateau. The black concave curve represents a sagittal cross-section of the medial tibial plateau while the black convex curve represents a sagittal sectional view of the lateral tibial plateau. In each diagram the solid and dashed blue circles represent two hypothetical positions of the medial femoral condyle and the lateral femoral condyle in the anterior-posterior direction. The two green dashed arrows are identical in length and represent

equal anterior-posterior translations of the femoral condylar centers in the medial and lateral compartments of the tibiofemoral joint. The orange dashed arrows represent the corresponding anterior-posterior translations of the tibiofemoral contact centers on the medial and lateral tibial plateaus. Equivalent translations of the centers of the femoral condyles result in a larger translation of the tibiofemoral contact center on the medial tibial plateau due to the concave shape of its surface. Note that the diagram presents a simplified description of condylar motion as it assumes that the medial and lateral femoral condyles are equal in size and neglects the involvement of a mobile meniscus.